



Value of susceptibility-weighted imaging in differentiating benign from malignant portal vein thrombosis

Chengling Huang^{1#}, Xixi Xiao^{2#}, Man Guo¹, Xianling Hu³, Chen Liu¹, Jian Wang¹, Huarong Zhang⁴, Xiaoming Li¹, Ping Cai¹

¹Department of Radiology, Southwest Hospital, Army Medical University (Third Military Medical University), Chongqing, China; ²Department of Oncology, Southwest Hospital, Army Medical University (Third Military Medical University), Chongqing, China; ³Communication Sergeant School, Army Engineering University of PLA, Chongqing, China; ⁴Institute of Pathology and Southwest Cancer Center, Southwest Hospital, Army Medical University (Third Military Medical University), Chongqing, China

Contributions: (I) Conception and design: C Huang, X Li, P Cai; (II) Administrative support: C Liu, J Wang; (III) Provision of study materials or patients: X Xiao, P Cai; (IV) Collection and assembly of data: C Huang, X Li; (V) Data analysis and interpretation: M Guo, X Hu; (VI) Pathology analysis: H Zhang; (VII) Manuscript writing: All authors; (VIII) Final approval of manuscript: All authors.

[#]These authors contributed equally to this work.

Correspondence to: Xiaoming Li; Ping Cai. Department of Radiology, Southwest Hospital, Army Medical University (Third Military Medical University), Chongqing, China. Email: 359261069@qq.com; 530305942 @qq.com.

Background: Many diseases are accompanied by portal vein thrombosis (PVT), and its nature is closely related to its prognosis and treatment. It is important to evaluate magnetic resonance imaging (MRI) parameters, including susceptibility-weighted imaging (SWI) and qualitative diffusion-weighted imaging (DWI), in the differentiation between benign and malignant PVT.

Methods: In this retrospective study, we collected clinical imaging data from 140 patients with PVTs characterized as benign or malignant based on enhanced MRI between January 2011 and April 2016 and retrospectively analyzed PVTs using SWI and DWI. There were 37 benign and 103 malignant PVTs. Image review was performed by 2 radiologists blinded to clinical information. The signal intensity (SI) of PVTs was recorded on SWI. The apparent diffusion coefficient (ADC) and the ratio of signal intensity (SIR) on SWI (SIR_{SWI}) and ADC (SIR_{ADC}) between the PVTs and the spinal cord were calculated. Finally, we generated receiver operating characteristic (ROC) curves to evaluate the efficacy of SIR_{SWI} and SIR_{ADC} for distinguishing benign and malignant PVTs.

Results: On SWI and DWI, 100.0% (36/36) and 80.5% (29/36) of benign PVTs were hypointense, respectively. For malignant PVTs on SWI and DWI, 99.0% (103/104) and 89.4% (93/104) were hyperintense, respectively. The SIR_{SWI} values of benign and malignant PVTs were 0.58 ± 0.13 and 0.88 ± 0.06 , respectively, representing a significant difference ($P < 0.001$). The SIR_{ADC} values of benign and malignant PVTs were 0.72 ± 0.32 and 0.62 ± 0.17 , respectively, representing a significant difference ($P = 0.034$). The area under the ROC curve (AUROC) for SIR_{SWI} [0.990; 95% confidence interval (CI): 0.971–1.000] was significantly higher than that for SIR_{ADC} (0.619; 95% CI: 0.500–0.737; $P < 0.001$). The SIR_{SWI} had a sensitivity of 100.0% and a specificity of 97.3% with a cutoff value of 0.749, while the SIR_{ADC} had a sensitivity of 45.9% and specificity of 83.3% with a cutoff value of 0.791.

Conclusions: The diagnostic performance of SWI is superior to that of DWI in the differentiation of benign and malignant PVTs.

Keywords: Benign; malignant; portal vein thrombosis (PVT); susceptibility-weighted imaging (SWI); diffusion-weighted imaging (DWI)

Submitted Apr 10, 2022. Accepted for publication Oct 08, 2022. Published online Oct 25, 2022.

doi: 10.21037/qims-22-350

View this article at: <https://dx.doi.org/10.21037/qims-22-350>

Introduction

Portal vein thrombosis (PVT) refers to complete or partial obstruction of the portal vein or its branches due to a variety of causes, including cirrhosis, malignancy, and non-hepatogenic diseases, such as splenectomy, gastrectomy, and pancreatitis (1-3). Notably, PVT can be either benign or malignant. A previous study has shown that malignant PVT is associated with hepatocellular carcinoma (HCC), which is unsuitable for surgical resection and liver transplantation (4). On the other hand, benign PVT often manifests with chronic liver disease, which can be treated with anticoagulant therapy (5). Consequently, accurate identification of the nature of PVT is imperative to determining the optimal treatment approach.

Although puncture biopsy remains the gold standard for differentiating benign from malignant PVTs, it is an invasive examination and has been associated with complications such as hemorrhage, sampling errors, and implantation metastasis. PVT can be differentiated using a variety of noninvasive techniques, including ultrasonography (6), computed tomography (CT) (7), and magnetic resonance imaging (MRI) (8,9). However, the number of studies evaluating MRI for this purpose remains limited (10). Based on our experience in daily practice, it is not always easy to distinguish benign from malignant PVTs. Therefore, a technique with high diagnostic accuracy is urgently needed to distinguish between benign and malignant PVTs.

Susceptibility-weighted imaging (SWI), an MRI technique based on T2* sequences, has been used to diagnose neurological disorders owing to its unique ability to detect intracranial iron deposition and hemorrhagic foci (11,12). Researchers have recently applied SWI technology to abdominal examinations because it is more sensitive in detecting siderotic nodules than are T2 and T2*-weighted imaging, particularly in patients with chronic liver disease or cirrhosis, and is more sensitive in detecting focal field inhomogeneity through the addition of phase information to the T2*-weighted imaging (13).

However, SWI sequences have rarely been used to diagnose PVT (14), and no study has yet compared diffusion-weighted imaging (DWI) and SWI in differentiating benign and malignant PVTs. Therefore, this

study aimed to compare the diagnostic efficacy of SWI and DWI in distinguishing benign from malignant PVTs. We present the following article in accordance with the STARD reporting checklist (available at <https://qims.amegroups.com/article/view/10.21037/qims-22-350/rc>).

Methods

Study population and selection criteria

The study was conducted in accordance with the Declaration of Helsinki (as revised in 2013). This study was approved by the Ethics Committee of Army Medical University (Third Military Medical University; No. KY2020280), and informed consent from patients was waived. From January 2011 to April 2016, we consecutively collected clinical data from 140 patients with PVTs, including their age, gender, surgical history (such as esophagogastric sclerotherapy, splenectomy, hepatectomy, and radiofrequency ablation), the coexistence of HCC and PVT, levels of alpha-fetoprotein (AFP), and presence of splenomegaly and ascites.

The inclusion criteria were as follows: (I) PVT present in the main branch and/or segmental branch; (II) complete clinical information; (III) availability of SWI, DWI, and enhanced MRI sequences; and (IV) an MRI quality adequate for analysis.

The exclusion criteria were as follows: (I) a PVT size too small for manual measurement; (II) incomplete clinical information; (III) lack of SWI and/or DWI sequences; and (IV) poor image quality.

Standard of reference for differentiating benign and malignant PVTs

The standards of reference for differentiating benign and malignant PVTs were those found in Shah *et al.* (15) and Catalano *et al.* (16). As it has been previously reported that vessel expansion of the portal vein can also be present in benign PVT (17), we did not propose to use the criterion of vessel expansion. Malignant PVT was considered if the following criteria were met and benign PVT if the criteria were not met: clear evidence of enhancement on dynamic

contrast-enhanced MRI during the arterial phase as defined by enhancement on the contrast-enhanced images when compared with baseline images ($\geq 15\%$).

MRI examination

All scans were performed on 3.0 T MRI system (Magnetom Trio, Siemens Medical Systems, Erlangen, Germany). The scans were obtained using sequences, including a single breath-hold T2-weighted imaging fast spin-echo sequence. The SWI sequence was acquired with the following parameters: flip angle = 20° , repetition time/time to echo (TR/TE) = 150/10 ms, a breath-hold = 16–21 s repeated 3 times, field of view = 380 mm \times 285 mm, matrix = 384 \times 187 mm, slice number = 30, and slice thickness = 5.5 mm. DWI imaging adopted breathing-triggered single-shot echo planar imaging technology, with b values of 0, 400, and 800 s/mm². The b values of 0 and 800 s/mm² were used to calculate the apparent diffusion coefficient (ADC) map monoexponentially. Gd-EOB-DTPA (Gadolinium-ethoxybenzyl-diethylenetriamine-pentaacetic acid) at a dose of 0.1 mL/kg was injected through the cubital vein at a speed of 1.0 mL/s. When the contrast agent reached the lower thoracic aorta, the patient performed a breath-hold for arterial phase scanning. Portal venous phase, transitional phase, and hepatobiliary phase scans were taken after a delay of 70 s, 2–5 min, and 15 min.

Imaging evaluation

All PVTs were assessed by 2 radiologists (XML and CLH with 8 and 6 years of abdominal imaging experience, respectively). Both radiologists were blinded to all patients' clinical information, and the intensity of thrombus was determined as hypointense or hyperintense relative to the liver on DWI (b=800 s/mm²). For quantitative analysis of SWI, all PVTs were measured using signal processing in Nuclear Magnetic Resonance software (SPIN version 1751, Spintech Software, Kharkiv, Ukraine, <https://spintechmri.com/research-software/>) at the Siemens workstation (Syngo. via) to measure the ADC on the ADC map. Each observer drew oval regions of interest (ROIs) in the thrombus and spinal cord as large as possible (≥ 10 mm²) with the same slice and regions (Figures 1,2). The signal intensity (SI) values of the thrombus and spinal cord on SWI and ADC obtained from the 2 observers were measured 3 times independently, and their mean values were recorded. Lastly, the ratios of signal intensity (SIR) on SWI (SIR_{SWI}) and

ADC (SIR_{ADC}) were calculated using the following formula: SI_{thrombus}/SI_{spinal cord}. Care was taken to avoid obvious artifacts, such as cerebrospinal fluid pulsation artifacts, respiratory motion artifacts, and magnetic susceptibility artifacts.

Statistical analysis

Statistical analyses were performed using SPSS 22.0 software (IBM Corp., Armonk, NY, USA). Variables with normal distributions are expressed as ($\bar{x} \pm s$), and pairwise comparisons were performed using the Student's *t* test. Nonnormally distributed continuous variables were analyzed using the Mann-Whitney test, while categorical variables were analyzed using the χ^2 -test. The statistical significance level was defined at $P < 0.05$. Receiver operating characteristic (ROC) curves were used to evaluate the diagnostic efficacy, and the point corresponding to the maximum Youden index (sensitivity + specificity - 1) was selected as the cutoff value. Comparison of the diagnostic efficiency of ROC curves was performed using the Delong test. Interobserver agreement for the intensity of thrombus was determined by calculating κ statistics as follows: $\kappa = 0$ –0.20, slight agreement; $\kappa = 0.21$ –0.40, fair agreement; $\kappa = 0.41$ –0.60, moderate agreement; $\kappa = 0.61$ –0.80, substantial agreement; and $\kappa = 0.81$ –1.00, almost perfect agreement.

Results

There were 37 benign and 103 malignant PVTs (124 males and 16 females), and benign and malignant PVTs co-occurred in 9 patients (Figure 3). The mean age of the cohort was 49.5 ± 11.2 years. There were statistically significant differences with regard to previous treatment history, AFP level, and the presence of combined HCC between benign and malignant PVTs ($P < 0.05$; Table 1).

For the evaluation of PVT signal, the result of interobserver agreement analysis indicated substantial agreement, intraclass correlation coefficients (ICCs) of signals evaluated by two radiologists on SWI and DWI were 0.75 and 0.65. On SWI and DWI, 100.0% (36/36) and 80.6% (29/36) of benign PVTs were hypointense, respectively. For malignant PVTs on SWI and DWI, 99.0% (103/104) and 89.4% (93/104) were hyperintense, respectively.

The mean SIR_{SWI} of benign and malignant PVTs were 0.58 ± 0.13 and 0.88 ± 0.06 (Figure 4), while the mean SIR_{ADC} of benign and malignant PVTs were 0.72 ± 0.32 and 0.62 ± 0.17 (Figure 5), respectively. There were significant

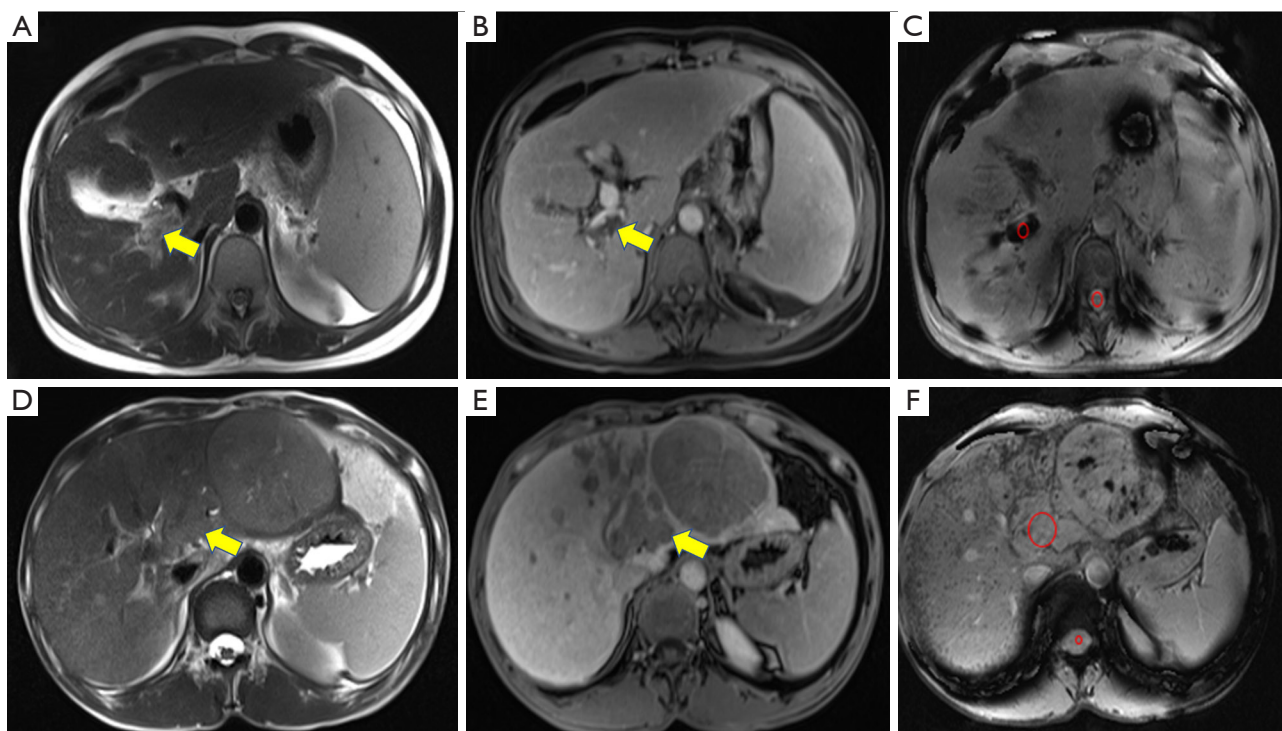


Figure 1 (A-C) Benign PVT in a 40-year-old woman. PVT (yellow arrow) appears hyperintense on T₂WI (A). PVT is also shown on the portal venous phase (yellow arrow) on enhanced MRI (B) and without enhancement during the arterial phase (not shown). The sample image of the ROI placement over the PVT and spinal cord (red circles) on SWI (C). (D-F) Malignant PVT in a 45-year-old man with HCC. PVT (yellow arrow) appears mildly hyperintense on T₂WI (D). PVT is also shown on the portal venous phase (yellow arrow) on enhanced MRI (E) and with enhancement during the arterial phase (not shown). The sample image of the ROI placement over the PVT and spinal cord (red circles) on SWI (F). PVT, portal vein thrombosis; T₂WI, T₂-weighted imaging; MRI, magnetic resonance imaging; ROI, region of interest; SWI, susceptibility-weighted imaging.

differences between benign and malignant PVTs on SWI [$t=18.651$; 95% confidence interval (CI): 0.273–0.337; $P<0.001$] and DWI ($t=-2.138$; 95% CI: -0.179–0.007; $P=0.034$). The area under the ROC curve (AUROC) for SIR_{SWI} (0.990; 95% CI: 0.971–1.000) was significantly higher than that for SIR_{ADC} (0.619; 95% CI: 0.500–0.737; $P<0.001$; *Figure 6*). The SIR_{SWI} had a sensitivity of 100.0% and a specificity of 97.3%, with a cutoff value of 0.749, while the SIR_{ADC} had a sensitivity of 45.9% and specificity of 83.3%, with a cutoff value of 0.791.

Discussion

Benign PVT is initially asymptomatic in the early phase; however, it potentially induces portal hypertension, which increases postoperative morbidity and mortality (18). Malignant PVT is associated with tumor staging, surgical

approach, and prognosis (19). This study shows that benign PVT is more likely to occur in patients with endoscopic injection sclerotherapy (EIS), splenectomy, hepatectomy, and radiofrequency ablation ($P<0.05$). These can lead to the development of benign PVT via portal venous endothelial injury, with increased portal vein pressure then causing slow or turbulent blood flow to pool in the portal venous system (20–22). Malignant PVTs are more likely to occur in patients with HCC and are caused directly by tumor invasion. Due to the different treatments and prognosis of benign and malignant PVTs, preoperative differentiation is of great importance.

Use of multimodal MRI, especially the ADC parameter, can help to distinguish between benign and malignant PVTs. Aumann *et al.* (23) reported that the ADC value can effectively differentiate benign and malignant PVTs, with sensitivity and specificity values of 80.0% and 72.7%,

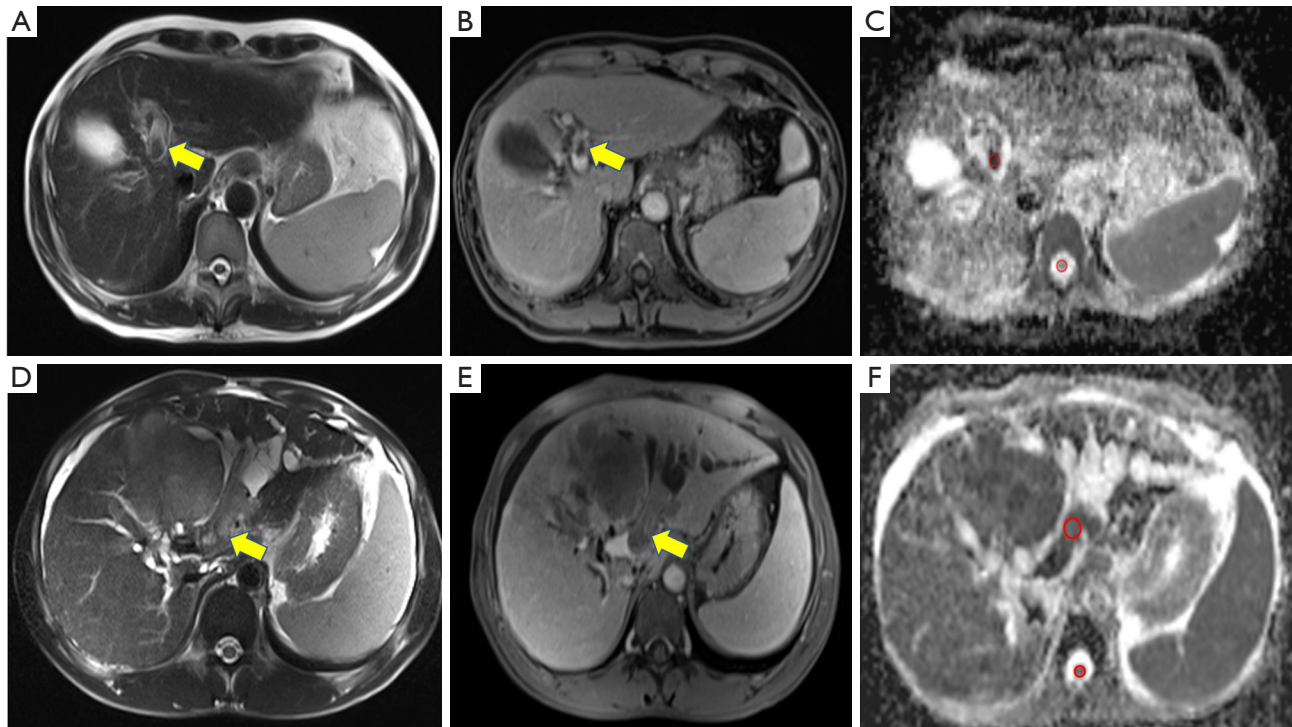


Figure 2 (A-C) Benign PVT in a 59-year-old man. PVT (yellow arrow) appears hypointense on T₂WI (A). PVT is also shown on the portal venous phase (yellow arrow) on enhanced MRI (B). The sample image of the ROI placement over the PVT and spinal cord (red circles) on the ADC map (C). (D-F) Malignant PVT in a 40-year-old man with cirrhosis and HCC. PVT (yellow arrow) appears mildly hyperintense on T₂WI (D). PVT is also shown on the portal venous phase (yellow arrow) on enhanced MRI (E). The sample image of the ROI placement over the PVT and spinal cord (red circles) on the ADC map (F). PVT, portal vein thrombosis; T₂WI, T₂-weighted imaging; MRI, magnetic resonance imaging; ROI, region of interest; ADC, apparent diffusion coefficient; HCC, hepatocellular carcinoma.

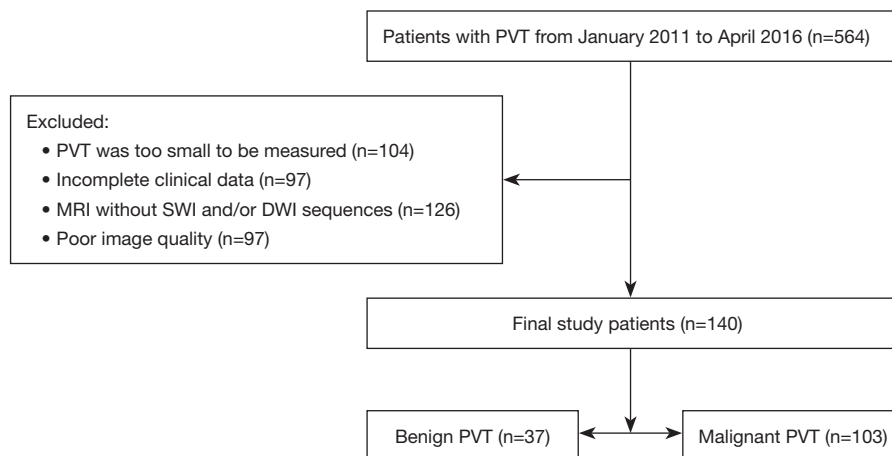


Figure 3 The flowchart of participants throughout the study. PVT, portal vein thrombosis; MRI, magnetic resonance imaging; SWI, susceptibility weighted imaging; DWI, diffusion weighted imaging.

Table 1 Summary of demographic data of the study population

Variable	Benign, n (%)	Malignant, n (%)	P value
Gender			0.642
Male	32 (86.5)	92 (89.3)	
Female	5 (13.5)	11 (10.7)	
Combined liver cirrhosis			0.141
No	7 (18.9)	10 (9.7)	
Yes	30 (81.1)	93 (90.3)	
Combined viral infection			0.790
No	5 (13.5)	18 (17.5)	
HBV	32 (86.5)	83 (80.6)	
HCV	0 (0.0)	2 (1.9)	
AFP level			<0.001
Negative	22 (59.5)	16 (15.5)	
Positive	15 (40.5)	87 (84.5)	
Combined HCC			<0.001
Absence	18 (48.6)	0 (0.0)	
Presence	19 (51.4)	103 (100.0)	
Treatment history			<0.001
No	9 (24.3)	72 (69.9)	
Yes	28 (75.7)	31 (30.1)	
Sclerotherapy	12	1	
Splenectomy	9	1	
Hepatectomy	6	21	
Radiofrequency ablation	12	9	
Splenomegaly			0.045
No	15 (40.5)	24 (23.3)	
Yes	22 (59.5)	79 (76.7)	
Ascites			0.391
No	16 (43.2)	53 (51.5)	
Yes	21 (56.8)	50 (48.5)	

AFP, alpha-fetoprotein; HBV, hepatitis B virus; HCV, hepatitis C virus; HCC, hepatocellular carcinoma.

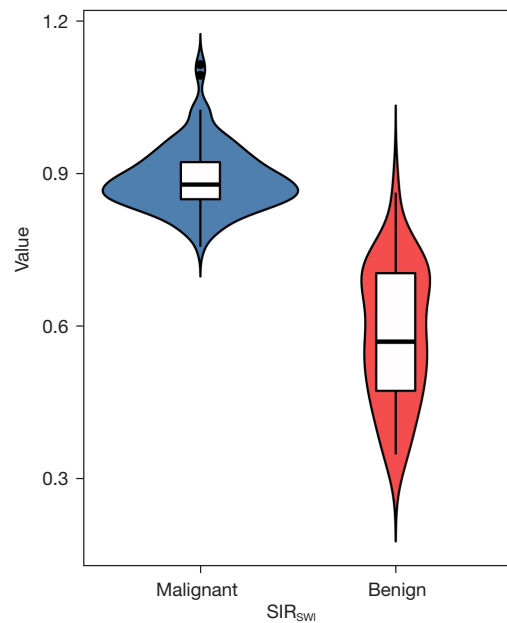


Figure 4 The SIR_{SWI} of benign and malignant PVTs. The mean SIR_{SWI} was statistically different between benign and malignant PVTs ($P<0.001$). SIR, signal intensity ratio; SWI, susceptibility-weighted imaging; PVT, portal vein thrombosis.

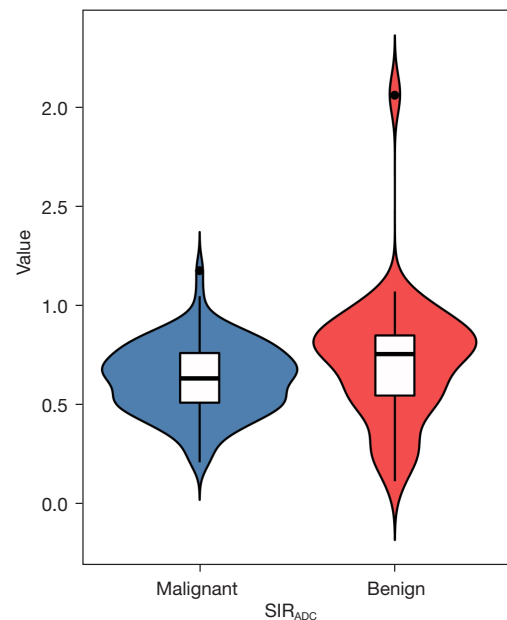


Figure 5 The SIR_{ADC} of benign and malignant PVTs. The mean SIR_{ADC} was statistically different between benign and malignant PVTs ($P=0.034$). SIR, signal intensity ratio; ADC, apparent diffusion coefficient; PVT, portal vein thrombosis.

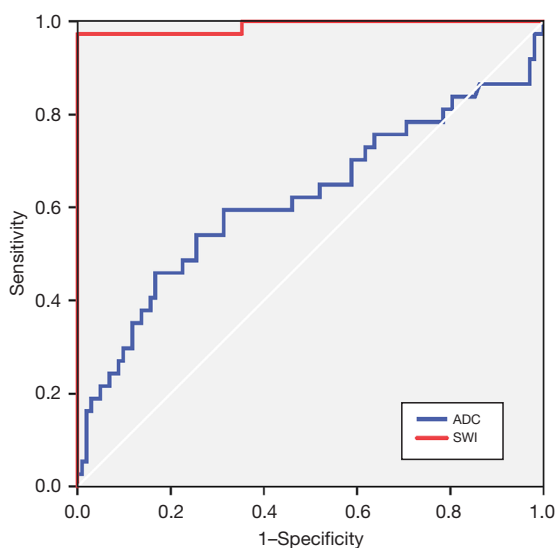


Figure 6 ROC curve analysis showing the diagnostic accuracy of SWI and DWI for differentiating benign and malignant PVTs. The area under the ROC curve for SIR_{SWI} (0.990; 95% CI: 0.971–1.000) was significantly higher than that for SIR_{ADC} (0.619; 95% CI: 0.500–0.737; $P < 0.001$). ROC, receiver operating characteristic; SWI, susceptibility-weighted imaging; DWI, diffusion-weighted imaging; PVT, portal vein thrombosis; CI, confidence interval; ADC, apparent diffusion coefficient.

respectively. However, Ahn *et al.* (24) reported an ADC value with a sensitivity of 22.2%, owing to wide range and considerable overlap of ADC, which is consistent with our result with a lower sensitivity (45.9%) for differentiating benign and malignant PVTs. The reason for this may be that the ADC value is influenced by the staging of thrombus, and benign PVT might have a low ADC similar to malignant PVT.

SWI involves nonionizing radiation and contrast-free technology, making it suitable for repeated examinations. To date, only a single study has examined the application value of SWI in distinguishing benign and malignant PVTs (14). However, this study had a small sample size ($n=42$), made no comparison with other MRI parameters, and calculated the phase values over the entire HCC, which might have introduced measurement error because of the significant heterogeneity of HCC. To our knowledge, a comparison of SWI and DWI for differentiating benign from malignant PVTs has not been performed previously. By comparing SIR_{SWI} and SIR_{ADC} , our research shows that the SWI

sequence can effectively distinguish benign and malignant PVTs (AUROC: 0.990), with a cutoff value of 0.749, which is significantly superior to the ADC parameter (AUROC: 0.619; $P < 0.001$). These results suggest that SWI is a promising tool that can be used to differentiate benign from malignant PVTs. This may be attributed to the higher sensitivity of SWI to PVT components.

SWI is an MRI sequence sensitive to compounds that distort the local magnetic field (e.g., calcium and iron) (25). The paramagnetic substances (e.g., deoxyhemoglobin and hemosiderin) increase the difference of magnetic susceptibility and shorten the $T2^*$ effect, and show low intensity on SWI (26). Benign PVT is characterized by high concentrations of paramagnetic substances, including deoxyhemoglobin and hemosiderin, so it appears as low intensity on SWI (14). However, malignant PVT is commonly caused by HCC invasion, which is mainly composed of tumor cells; however, malignant PVT is usually caused by the invasion of HCC, which is mainly composed of tumor cells. Like HCC, malignant PVT also undergoes deionization, and shows high signal on SWI (27,28).

This study had some limitations. First, as our study was single-center and retrospective in design, we lack external validation data. Second, we did not compare the efficacy of SWI and CT in differentiating benign and malignant PVTs, and so we will collect CT data in the future to verify the value of the 2 techniques in differentiating benign and malignant PVTs. Third, the ROI was manually contoured, and the SI obtained does not accurately reflect the entire PVT. Finally, the SI of the PVTs and HCC lesions in the same patients was not compared on SWI and ADC sequences.

Conclusions

In conclusion, SWI is noninvasive technique that uses nonionizing radiation, and its diagnostic performance is comparable or superior to that of DWI in the differentiation of benign and malignant PVTs.

Acknowledgments

Funding: This study was supported by the National Key Research and Development Program of China (Nos. 2016YFC0107101 and 2016YFC0107109) and the General Program of National Natural Science Foundation of Chongqing (No. CSTB2022NSCQ-MSX1371).

Footnote

Reporting Checklist: The authors have completed the STARD reporting checklist. Available at <https://qims.amegroups.com/article/view/10.21037/qims-22-350/rc>

Conflicts of Interest: All authors have completed the ICMJE uniform disclosure form (available at <https://qims.amegroups.com/article/view/10.21037/qims-22-350/coif>). All authors report that this study was supported by the National Key Research and Development Program of China (Nos. 2016YFC0107101 and 2016YFC0107109) and the General Program of National Natural Science Foundation of Chongqing (No. CSTB2022NSCQ-MSX1371). The authors have no other conflicts of interest to declare.

Ethical Statement: The authors are accountable for all aspects of the work by ensuring that questions related to the accuracy or integrity of any part of the work are appropriately investigated and resolved. The study was conducted in accordance with the Declaration of Helsinki (as revised in 2013). The study was approved by the Ethics Committee of Army Medical University (Third Military Medical University; No. KY2020280), and individual consent for this retrospective study was waived.

Open Access Statement: This is an Open Access article distributed in accordance with the Creative Commons Attribution-NonCommercial-NoDerivs 4.0 International License (CC BY-NC-ND 4.0), which permits the non-commercial replication and distribution of the article with the strict proviso that no changes or edits are made and the original work is properly cited (including links to both the formal publication through the relevant DOI and the license). See: <https://creativecommons.org/licenses/by-nc-nd/4.0/>.

References

- Valla DC, Condat B. Portal vein thrombosis in adults: pathophysiology, pathogenesis and management. *J Hepatol* 2000;32:865-71.
- De Stefano V, Martinelli I. Splanchnic vein thrombosis: clinical presentation, risk factors and treatment. *Intern Emerg Med* 2010;5:487-94.
- Chawla Y, Duseja A, Dhiman RK. Review article: the modern management of portal vein thrombosis. *Aliment Pharmacol Ther* 2009;30:881-94.
- Takizawa D, Kakizaki S, Sohara N, Sato K, Takagi H, Arai H, Katakai K, Kojima A, Matsuzaki Y, Mori M. Hepatocellular carcinoma with portal vein tumor thrombosis: clinical characteristics, prognosis, and patient survival analysis. *Dig Dis Sci* 2007;52:3290-5.
- Ogren M, Bergqvist D, Björck M, Acosta S, Eriksson H, Sternby NH. Portal vein thrombosis: prevalence, patient characteristics and lifetime risk: a population study based on 23,796 consecutive autopsies. *World J Gastroenterol* 2006;12:2115-9.
- Chammas MC, Oliveira AC, D Ávila MJ, Moraes PH, Takahashi MS. Characterization of Malignant Portal Vein Thrombosis with Contrast-Enhanced Ultrasonography. *Ultrasound Med Biol* 2019;45:50-5.
- Rossi S, Ghittoni G, Ravetta V, Torello Viera F, Rosa L, Serassi M, Scabini M, Vercelli A, Tinelli C, Dal Bello B, Burns PN, Calliada F. Contrast-enhanced ultrasonography and spiral computed tomography in the detection and characterization of portal vein thrombosis complicating hepatocellular carcinoma. *Eur Radiol* 2008;18:1749-56.
- Kim JH, Lee JM, Yoon JH, Lee DH, Lee KB, Han JK, Choi BI. Portal Vein Thrombosis in Patients with Hepatocellular Carcinoma: Diagnostic Accuracy of Gadoteric Acid-enhanced MR Imaging. *Radiology* 2016;279:773-83.
- Gawande R, Jalaiean H, Niendorf E, Olgun D, Krystosek L, Rubin N, Spilseth B. MRI in differentiating malignant versus benign portal vein thrombosis in patients with hepatocellular carcinoma: Value of post contrast imaging with subtraction. *Eur J Radiol* 2019;118:88-95.
- Choi JY, Lee JM, Sirlin CB. CT and MR imaging diagnosis and staging of hepatocellular carcinoma: part I. Development, growth, and spread: key pathologic and imaging aspects. *Radiology* 2014;272:635-54.
- Haacke EM, Mittal S, Wu Z, Neelavalli J, Cheng YC. Susceptibility-weighted imaging: technical aspects and clinical applications, part 1. *AJNR Am J Neuroradiol* 2009;30:19-30.
- Okada T, Fujimoto K, Fushimi Y, Akasaka T, Thuy DHD, Shima A, Sawamoto N, Oishi N, Zhang Z, Funaki T, Nakamoto Y, Murai T, Miyamoto S, Takahashi R, Isa T. Neuroimaging at 7 Tesla: a pictorial narrative review. *Quant Imaging Med Surg* 2022;12:3406-35.
- Chen W, DelProposto Z, Wu D, Wang J, Jiang Q, Xuan S, Ye Y, Zhang Z, Hu J. Improved siderotic nodule detection in cirrhosis with susceptibility-weighted magnetic resonance imaging: a prospective study. *PLoS One* 2012;7:e36454.
- Li C, Hu J, Zhou D, Zhao J, Ma K, Yin X, Wang J.

- Differentiation of bland from neoplastic thrombus of the portal vein in patients with hepatocellular carcinoma: application of susceptibility-weighted MR imaging. *BMC Cancer* 2014;14:590.
15. Shah ZK, McKernan MG, Hahn PF, Sahani DV. Enhancing and expansile portal vein thrombosis: value in the diagnosis of hepatocellular carcinoma in patients with multiple hepatic lesions. *AJR Am J Roentgenol* 2007;188:1320-3.
 16. Catalano OA, Choy G, Zhu A, Hahn PF, Sahani DV. Differentiation of malignant thrombus from bland thrombus of the portal vein in patients with hepatocellular carcinoma: application of diffusion-weighted MR imaging. *Radiology* 2010;254:154-62.
 17. Sandrasegaran K, Tahir B, Nutakki K, Akisik FM, Bodanapally U, Tann M, Chalasani N. Usefulness of conventional MRI sequences and diffusion-weighted imaging in differentiating malignant from benign portal vein thrombus in cirrhotic patients. *AJR Am J Roentgenol* 2013;201:1211-9.
 18. Kuboki S, Shimizu H, Ohtsuka M, Kato A, Yoshitomi H, Furukawa K, Takayashiki T, Takano S, Okamura D, Suzuki D, Sakai N, Kagawa S, Miyazaki M. Incidence, risk factors, and management options for portal vein thrombosis after hepatectomy: a 14-year, single-center experience. *Am J Surg* 2015;210:878-85.e2.
 19. Reig M, Forner A, Rimola J, Ferrer-Fàbrega J, Burrel M, Garcia-Criado Á, Kelley RK, Galle PR, Mazzaferro V, Salem R, Sangro B, Singal AG, Vogel A, Fuster J, Ayuso C, Bruix J. BCLC strategy for prognosis prediction and treatment recommendation: The 2022 update. *J Hepatol* 2022;76:681-93.
 20. Swinson B, Waters PS, Webber L, Nathanson L, Cavallucci DJ, O'Rourke N, Bryant RD. Portal vein thrombosis following elective laparoscopic splenectomy: incidence and analysis of risk factors. *Surg Endosc* 2022;36:3332-9.
 21. Qi X, Han G, Fan D. Management of portal vein thrombosis in liver cirrhosis. *Nat Rev Gastroenterol Hepatol* 2014;11:435-46.
 22. Kumar A, Sharma P, Arora A. Review article: portal vein obstruction--epidemiology, pathogenesis, natural history, prognosis and treatment. *Aliment Pharmacol Ther* 2015;41:276-92.
 23. Aumann EK, Server S, Koyuncu Sokmen B, Oz A, Namal E, Gurcan NI, Balci NC, Tokat Y. Diagnostic performances of intravoxel incoherent motion and conventional diffusion-weighted imaging in the differential diagnosis of benign and malignant portal vein thrombus. *Abdom Radiol (NY)* 2018;43:2270-6.
 24. Ahn JH, Yu JS, Cho ES, Chung JJ, Kim JH, Kim KW. Diffusion-Weighted MRI of Malignant versus Benign Portal Vein Thrombosis. *Korean J Radiol* 2016;17:533-40.
 25. Haller S, Haacke EM, Thurnher MM, Barkhof F. Susceptibility-weighted Imaging: Technical Essentials and Clinical Neurologic Applications. *Radiology* 2021;299:3-26.
 26. Mittal S, Wu Z, Neelavalli J, Haacke EM. Susceptibility-weighted imaging: technical aspects and clinical applications, part 2. *AJNR Am J Neuroradiol* 2009;30:232-52.
 27. Chen W, DelProposto Z, Liu W, Kassir M, Wang Z, Zhao J, Xie B, Wen Y, Wang J, Hu J. Susceptibility-weighted imaging for the noncontrast evaluation of hepatocellular carcinoma: a prospective study with histopathologic correlation. *PLoS One* 2014;9:e98303.
 28. Sorrentino P, D'Angelo S, Ferbo U, Micheli P, Bracigliano A, Vecchione R. Liver iron excess in patients with hepatocellular carcinoma developed on non-alcoholic steato-hepatitis. *J Hepatol* 2009;50:351-7.

Cite this article as: Huang C, Xiao X, Guo M, Hu X, Liu C, Wang J, Zhang H, Li X, Cai P. Value of susceptibility-weighted imaging in differentiating benign from malignant portal vein thrombosis. *Quant Imaging Med Surg* 2023;13(4):2688-2696. doi: 10.21037/qims-22-350